ISSN 0021-3640, JETP Letters, 2008, Vol. 88, No. 2, pp. 85–90. © Pleiades Publishing, Ltd., 2008.
Original Russian Text © V.M. Aul'chenko, R.R. Akhmetshin, B.Sh. Banzarov, L.M. Barkov, N.S. Bashtovoi, A.E. Bondar', A.V. Bragin, A.A. Grebenyuk, D.N. Grigor'ev, D.A. Epifanov, A.S. Zaitsev, F.V. Ignatov, V.F. Kazanin, S.V. Karpov, I.A. Koop, P.P. Krokovny, A.S. Kuz'min, I.B. Logashenko, P.A. Lukin, K.Yu. Mikhailov, I.N. Nesterenko, A.V. Otboev, V.S. Okhapkin, E.A. Perevedentsev, A.S. Popov, S.I. Redin, A.A. Ruban, N.M. Ryskulov, A.L. Sibidanov, V.P. Smakhtin, I.G. Snopkov, E.P. Solodov, G.V. Fedotovich, B.I. Khazin, Yu.M. Shatunov, B.A. Shvarts, S.I. Eidel'man, Yu.V. Yudin, 2008, published in Pis'ma v Zhurnal Éksperimental'noĭ i Teoreticheskoĭ Fiziki, 2008, Vol. 88, No. 2, pp. 93–98.

Search for the $\phi \longrightarrow \pi^+\pi^-\gamma\gamma$ and $\phi \longrightarrow \pi^+\pi^-\eta$ Decays with the CMD-2 Detector

V. M. Aul'chenko[a, b], R. R. Akhmetshin[a], B. Sh. Banzarov[a], L. M. Barkov[a, b], N. S. Bashtovoi[a], A. E. Bondar'[a], A. V. Bragin[a], A. A. Grebenyuk[a], D. N. Grigor'ev[a–c], D. A. Epifanov[a], A. S. Zaitsev[a, b], F. V. Ignatov[a], V. F. Kazanin[a, b], S. V. Karpov[a], I. A. Koop[a, b], P. P. Krokovny[a, b], A. S. Kuz'min[a, b], I. B. Logashenko[a, d], P. A. Lukin[a], K. Yu. Mikhailov[a], I. N. Nesterenko[a, b], A. V. Otboev[a], V. S. Okhapkin[a], E. A. Perevedentsev[a, b], A. S. Popov[a], S. I. Redin[a], A. A. Ruban[a], N. M. Ryskulov[a], A. L. Sibidanov[a], V. P. Smakhtin[e], I. G. Snopkov[a], E. P. Solodov[a, b], G. V. Fedotovich[a, b], B. I. Khazin[a, b], Yu. M. Shatunov[a], B. A. Shvarts[a, b], S. I. Eidel'man[a, b], and Yu. V. Yudin[a]

[a] *Budker Institute of Nuclear Physics, Siberian Branch, Russian Academy of Sciences, pr. Akademika Lavrent'eva 11, Novosibirsk, 630090 Russia*
e-mail: epifanov@inp.nsk.su
[b] *Novosibirsk State University, ul. Pirogova 2, Novosibirsk, 630090 Russia*
[c] *Novosibirsk State Technical University, Novosibirsk, 630092 Russia*
[d] *Boston University, Boston, MA 02215, USA*
[e] *Weizmann Institute of Science, 76100 Rehovot, Israel*

Received June 17, 2008

The $\phi \longrightarrow \pi^+\pi^-\gamma\gamma$ and $\phi \longrightarrow \pi^+\pi^-\eta$ decays are sought in the experimental data obtained with the CMD-2 detector in the region of the ϕ-meson resonance. Upper limits $\mathcal{B}(\phi \longrightarrow \pi\pi\gamma\gamma) < 1.2 \times 10^{-4}$ and $\mathcal{B}(\phi \longrightarrow \pi\pi\eta) < 6.1 \times 10^{-5}$ (both at a C.L. of 90%) are determined for the branching ratios of these decays.

PACS numbers: 13.25.-k, 13.66.-a, 14.40.Ev

DOI: 10.1134/S0021364008140038

INTRODUCTION

Investigations of the rare decays of light vector mesons are important for the understanding of the structure of light hadrons and the dynamics of their interactions. New information on these decays makes it possible to determine the limits of the applicability of the vector dominance model and SU(3) symmetry, as well as to test various phenomenological models of light hadrons. For this reason, the investigation of the rare decays of light vector mesons was one of the main aims of the experiments with the CMD-2 detector [1] that were carried out at the Budker Institute of Nuclear Physics from 1992 to 2000 at the VEPP-2M electron–positron collider [2] in the cm energy range 0.36–1.4 GeV. The experimental data with a total luminosity of about 14 pb^{-1} obtained in the region of the ϕ-meson resonance allow the analysis of the rare decay modes with branching ratios of 10^{-4}–10^{-5}.

The aim of this work is to seek the $\phi \longrightarrow \pi^+\pi^-\gamma\gamma$ and $\phi \longrightarrow \pi^+\pi^-\eta$ decays. According to [3], the $\phi \longrightarrow \rho^0\gamma\gamma$, $\rho^0 \longrightarrow \pi^+\pi^-$ decay can proceed through the intermediate states η and η'. This mechanism gives rise to an increase in the probability of the $\phi \longrightarrow \rho^0\gamma\gamma$ decay as compared to the prediction of chiral perturbation theory for vector mesons [4]. A branching ratio of $\mathcal{B}(\phi \longrightarrow \rho^0\gamma\gamma) = 1.3 \times 10^{-4}$ was predicted in [3].

According to [5], the $\phi \longrightarrow \pi^+\pi^-\eta$ decay must proceed through the intermediate state $\rho\eta$. The G parity is broken in this decay; hence, its branching ratio must be on the order of the value for the $\phi \longrightarrow \pi^+\pi^-$ decay, i.e., 10^{-4}. However, Karnakov [5] predicted that this decay is suppressed by additional two orders of magnitude and is $\mathcal{B} = 0.35 \times 10^{-6}$. The measurement of $\mathcal{B}(\phi \longrightarrow \pi^+\pi^-\eta)$ can clarify the features of the mechanism of this decay.

CMD-2 DETECTOR

The cryogenic magnetic detector CMD-2 allows the detection of the charged particles and photons and precise measurements of their parameters. The layout of the detector is shown in Fig. 1. The coordinates, emission angles, and momenta of charged particles are measured in the coordinate system of the detector. This system consists of the (*2*) drift and (*3*) Z chambers placed in a magnetic field of 10 kG created by (*4*) a supercon-

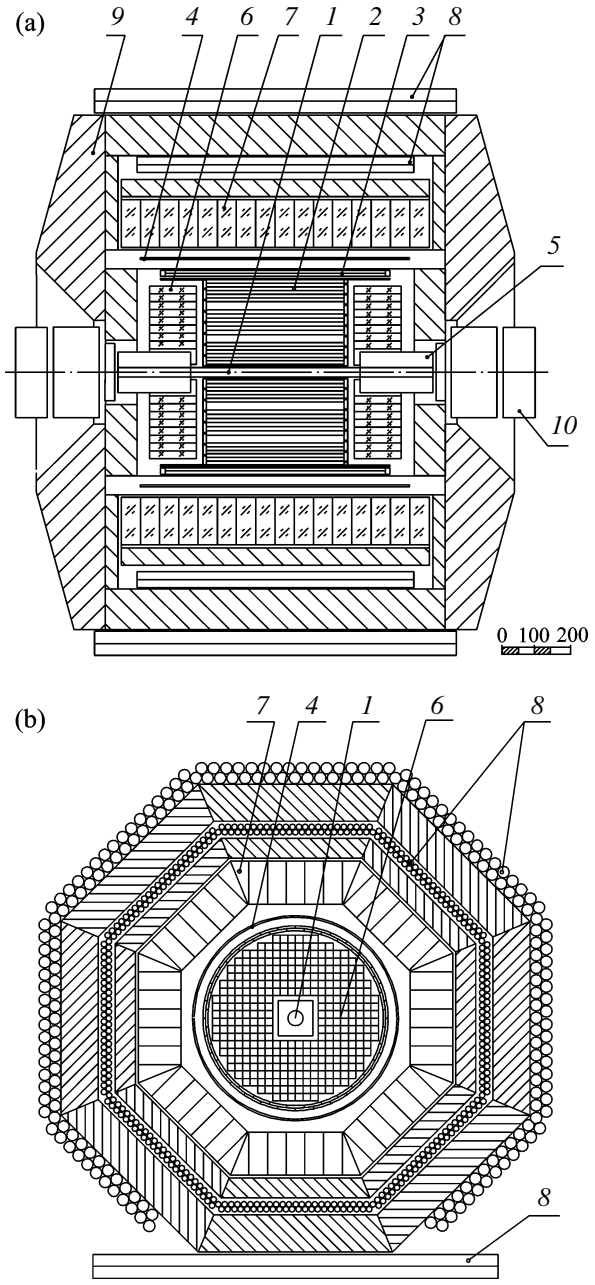

Fig. 1. CMD-2 detector in the (a) *R–Z* and (b) φ projections: (*1*) vacuum chamber, (*2*) drift chamber, (*3*) *Z* chamber, (*4*) main superconducting solenoid, (*5*) compensating solenoid, (*6*) endcap calorimeter based on the BGO crystals, (*7*) cylindrical calorimeter based on the CsI crystals, (*8*) muon system, (*9*) magnet yoke, and (*10*) quadrupole lenses.

ducting solenoid. The (*7*) cylindrical and (*6*) endcap electromagnetic calorimeters based on CsI and BGO scintillation crystals, respectively, ensure both the measurement of the energy and angles of photons and the separation of electrons and hadrons. Path system *8* is used to separate muons and hadrons. In this work, we seek the $\phi \longrightarrow \pi^+\pi^-\gamma\gamma$ and $\phi \longrightarrow \pi^+\pi^-\eta$ decays in the experimental data with a total luminosity of about 11 pb^{-1} collected on the CMD-2 detector in the region of the φ-meson resonance in the range $2E$ = 984–1060 MeV of the cm energy of e^+e^- beams.

EVENT SELECTION

The events of the $\phi \longrightarrow \pi^+\pi^-\gamma\gamma$ and $\phi \longrightarrow \pi^+\pi^-\eta$ decays, where the η meson is identified through the two-photon decay mode $\eta \longrightarrow \gamma\gamma$, contain two charged pions and two photons in the final state. The resonance background for the desired processes comes from the events of the φ-meson decays:

(i) $\phi \longrightarrow K^+K^-$, where the sources of photons are the kaon decay products; in addition, spurious photon clusters appear due either to the nuclear interaction of the kaons with the detector material or to the random triggering of the calorimeter;

(ii) $\phi \longrightarrow K_SK_L$, $K_S \longrightarrow \pi^+\pi^-$, where the spurious photon clusters appear due to the nuclear interaction of K_L with the calorimeter material;

(iii) $\phi \longrightarrow \pi^+\pi^-\pi^0$, $\pi^0 \longrightarrow \gamma\gamma$;

(iv) $\phi \longrightarrow \eta\gamma$, $\eta \longrightarrow \pi^+\pi^-\gamma$ or $\eta \longrightarrow \pi^+\pi^-\pi^0$, $\pi^0 \longrightarrow \gamma\gamma$.

The nonresonance background is determined by the following processes:

(i) $e^+e^- \longrightarrow e^+e^-\gamma(\gamma)$,

(ii) $e^+e^- \longrightarrow \mu^+\mu^-\gamma(\gamma)$,

(iii) $e^+e^- \longrightarrow \rho\gamma(\gamma) \longrightarrow \pi^+\pi^-\gamma(\gamma)$, and

(iv) $e^+e^- \longrightarrow \pi^+\pi^-\pi^0\pi^0$.

The search for the $\phi \longrightarrow \pi^+\pi^-\gamma\gamma$ and $\phi \longrightarrow \pi^+\pi^-\eta$ events was performed in two stages. In the first stage, events with two charged particles and two photons were selected in which the $\phi \longrightarrow \pi^+\pi^-\pi^0$ and $\phi \longrightarrow \eta\gamma(\eta \longrightarrow \pi^+\pi^-\gamma, \eta \longrightarrow \pi^+\pi^-\pi^0)$ events dominate. The tracks and photons must satisfy the following criteria.

—For each track, the spreads of the hits with respect to the track projections on the (*R*–φ) and (*R–Z*) planes should be $\sigma_R < 0.1$ cm and $\sigma_Z < 3$ cm, respectively [in this case, the spatial resolutions of the drift chamber in the (*R*–φ) and (*R–Z*) planes are $\bar{\sigma}_R \simeq 0.025$ cm and $\bar{\sigma}_Z \simeq 0.4$ cm, respectively].

—The track angles in the *R*–φ projection satisfy the condition $|\pi - |\varphi_+ - \varphi_-|| > 0.1$, which is used to suppress the $e^+e^- \longrightarrow e^+e^-(\gamma)$ background events, and the angle between the tracks should be $\psi > 0.1$ in order to suppress the photon conversion events on the wall of the vacuum chamber of the detector.

—A charged particle should intersect all of the layers of the drift and *Z* chambers; this is ensured by the condition $|\pi/2 - \theta_\pm| < 0.67$ for the polar angle of the track.

—The minimum distance from the track to the beam axis in the R–φ plane is $R_{\min} < 0.2$ cm, and the distance between the track point nearest to the beam axis and the meeting point along the beam axis is $|Z_{\text{trk}}| < 10$ cm.

—To suppress the events with misidentified tracks, the absolute value of the momentum of the charged particle must satisfy the condition $P_{\pm} < 550$ MeV/c.

—To suppress the events with electrons and positrons in the final state, the ratio of the energy release in a cluster associated with a track to the momentum must satisfy the condition $E_{\text{clus}\pm}/P_{\pm} < 0.8$.

—The ionization losses of the charged particle per unit length in the drift chamber satisfy the condition $dE/dx < 2(dE/dx)_{\text{mip}}$, where $(dE/dx)_{\text{mip}}$ are the ionization losses of the minimum ionizing particle per unit length. This condition ensures the suppression of the background events with charged kaons.

—It is required that photons with energies $E_{\gamma 1,2} > 50$ MeV enter the cylindrical calorimeter of the detector; this is ensured by the condition $|\pi/2 - \theta_{\gamma 1,2}| < 0.67$ for the polar angle of the photons.

Events with tracks and photons that do not satisfy the above criteria in addition to the selected two tracks and two photons are also analyzed. To suppress the background from the $\phi \longrightarrow K^+K^-$ and $\phi \longrightarrow K_SK_L$ decays, we exclude the events satisfying the conditions $P_+ < 140$ MeV/c^2, $P_- < 140$ MeV/c^2, and 380 MeV/c^2 < $(P_+ + P_-) < 470$ MeV/c^2. To exclude the events with clusters produced by neutrons, which can appear in the nuclear interaction of pions, the angle between the photon cluster and the nearest cluster associated with a charged particle should satisfy the condition $\Delta\psi_{\gamma-\text{trk}} > 0.5$.

To improve the resolutions in the angles and momenta of the particles, we use the kinematic reconstruction of an event with the use of the energy and momentum conservation laws:

$$\begin{aligned} E_{\pi^+} + E_{\pi^-} + E_{\gamma 1} + E_{\gamma 2} &= 2E, \\ \mathbf{P}_{\pi^+} + \mathbf{P}_{\pi^-} + \mathbf{P}_{\gamma 1} + \mathbf{P}_{\gamma 2} &= 0. \end{aligned} \quad (1)$$

Additional selection with the χ^2 parameter of the kinematic reconstruction ensures a significant suppression of the resonance background from misreconstructed $\phi \longrightarrow K\bar{K}$ events with a high sensitivity to the signal events. Figure 2 shows the distribution of the selected events in the $(M_{\gamma\gamma}, E_{\gamma\max})$ plane, where $M_{\gamma\gamma}$ is the invariant mass of the photons and $E_{\gamma\max}$ is the energy of the photon with the highest energy.

In the second stage, the events are analyzed in the $(M_{\gamma\gamma}, E_{\gamma\max})$ plane. We consider the following four regions:

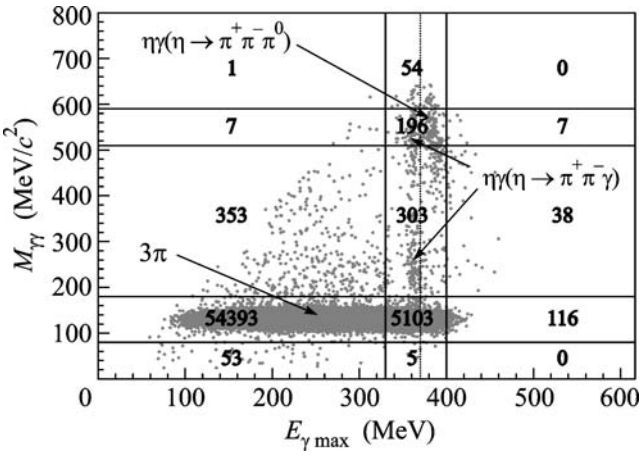

Fig. 2. Distribution of experimental events in the $(M_{\gamma\gamma}, E_{\gamma\max})$ plane. The plane is divided into 15 rectangular regions; the numbers of the events in these regions are given.

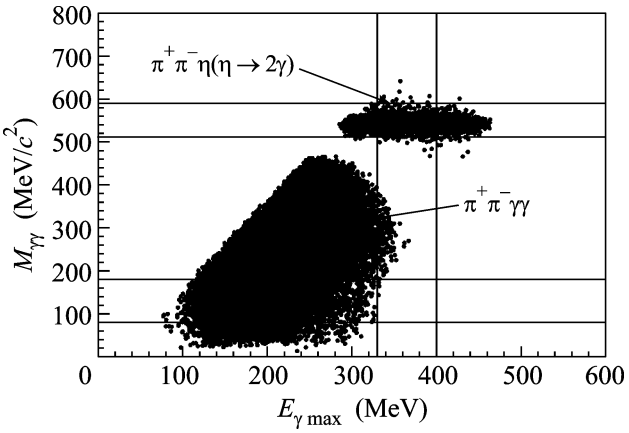

Fig. 3. Distribution of the simulated $\phi \longrightarrow \pi^+\pi^-\gamma\gamma$ and $\phi \longrightarrow \rho^0\eta \longrightarrow \pi^+\pi^-\eta$ events in the $M_{\gamma\gamma}$–$E_{\gamma\max}$ plane.

(i) 80 MeV/$c^2 < M_{\gamma\gamma} < 180$ MeV/c^2, where the $\phi \longrightarrow \pi^+\pi^-\pi^0$ events dominate.

(ii) $M_{\gamma\gamma} > 180$ MeV/c^2 and 330 MeV $< E_{\gamma\max} <$ 400 MeV, where the $\phi \longrightarrow \eta\gamma(\eta \longrightarrow \pi^+\pi^-\gamma, \eta \longrightarrow \pi^+\pi^-\pi^0)$ events dominate. To select the $\phi \longrightarrow \eta\gamma(\eta \longrightarrow \pi^+\pi^-\gamma)$ events in this region, we use the additional criterion $E_{\gamma\max} < 370$ MeV, which is shown by the dashed line in Fig. 2.

(iii) 180 MeV/$c^2 < M_{\gamma\gamma} < 510$ MeV/c^2 and $E_{\gamma\max} <$ 330 MeV, where most events of the desired $\phi \longrightarrow \pi^+\pi^-\gamma\gamma$ decay appear (see also Fig. 3).

Some $\phi \longrightarrow \pi^+\pi^-\pi^0$ events are also in this region (about 2×10^{-6} of their total number).

Table 1. Detection efficiencies

Decay	Mechanism	Efficiency
3π	$\rho\pi$	$\varepsilon_{3\pi}^{(1)} = (2.44 \pm 0.02)\%$
		$\varepsilon_{3\pi}^{(2)} = (6.0 \pm 2.4) \times 10^{-6}$
		$\varepsilon_{3\pi}^{(3)} = (2.0 \pm 1.4) \times 10^{-6}$
$\eta\gamma$	$\eta \longrightarrow \pi\pi\gamma$	$\varepsilon_{\eta\gamma}^{(2)} = (2.41 \pm 0.02)\%$
		$\varepsilon_{\eta\gamma}^{(4)} = (5.0 \pm 2.2) \times 10^{-6}$
$\pi\pi\gamma\gamma$	η	$\varepsilon_{\pi\pi\gamma\gamma}^{(3)} = (2.35 \pm 0.02)\%$
$\pi^+\pi^-\eta$	$\rho^0\eta$	$\varepsilon_{\pi\pi\eta}^{(4)} = (3.77 \pm 0.03)\%$

Table 2. Approximation results

Decay	σ_B^f, nb	$\mathcal{B}^f$, 10^{-5}
$\eta\gamma$ ($\eta \longrightarrow \pi\pi\gamma$)	2.77 ± 0.18	66.1 ± 4.3
$\pi\pi\gamma\gamma$	0.193 ± 0.186	4.6 ± 4.4
$\pi\pi\eta$ ($\eta \longrightarrow \gamma\gamma$)	0.042 ± 0.035	2.5 ± 2.1

(iv) 510 MeV/c^2 < $M_{\gamma\gamma}$ < 590 MeV/c^2 and $E_{\gamma\max}$ < 330 MeV or $E_{\gamma\max}$ > 400 MeV, where about half of the events of the desired $\phi \longrightarrow \pi^+\pi^-\eta$ ($\eta \longrightarrow \gamma\gamma$) decay appear (see Fig. 3).

Figure 3 shows the distribution of the simulated $\phi \longrightarrow \pi^+\pi^-\gamma\gamma$ and $\phi \longrightarrow \pi^+\pi^-\eta$ events in the ($M_{\gamma\gamma}$, $E_{\gamma\max}$) plane. For this simulation, the matrix element for the $\phi \longrightarrow \pi^+\pi^-\gamma\gamma$ decay is written according to [3], where the decay was assumed to proceed through the intermediate virtual state η ($M_{\pi^+\pi^-} > 550$ MeV/c^2) with the formation of the final state $\rho^0\gamma\gamma$. The $\phi \longrightarrow \pi^+\pi^-\eta$ decay is simulated under the assumption of the production of the $\rho^0\eta$ intermediate state. According to Fig. 3, about half of the $\phi \longrightarrow \pi^+\pi^-\eta$ events are in the region 330 MeV < $E_{\gamma\max}$ < 400 MeV. However, this region is not used for seeking this decay because of the large background from the $\phi \longrightarrow \eta\gamma(\eta \longrightarrow \pi^+\pi^-\gamma, \eta \longrightarrow \pi^+\pi^-\pi^0)$ decays. To suppress the $\phi \longrightarrow \pi^+\pi^-\pi^0$ events in region (iii), we apply the following additional constraint on the missing mass for the $\pi^+\pi^-$ system in this region: $M_{\text{miss}}(\pi^+\pi^-) = \sqrt{4E(E - E_{\pi^+} - E_{\pi^-}) + 2(E_{\pi^+}E_{\pi^-} - \mathbf{P}_{\pi^+}\mathbf{P}_{\pi^-}) + 2m_\pi^2} >$ 300 MeV/c^2. Note that the events of the $\phi \longrightarrow \eta'\gamma \longrightarrow \pi\pi\gamma\gamma$ decay through the η' intermediate state (real or virtual) locate in the region with $M_{\text{miss}}(\pi^+\pi^-)$ < 300 MeV/c^2 and are also suppressed by the selection rule for $M_{\text{miss}}(\pi^+\pi^-)$. The numbers of the selected events in the regions are $N^{(1)} = 58\,207$, $N^{(2)} = 285$, $N^{(3)} = 112$, and $N^{(4)} = 13$.

DETERMINATION OF THE DECAY PROBABILITIES

The number of events in the ith region (i = 1–4) at each of the 16 points of energy E is calculated by the formula

$$N_{\text{calc}}^{(i)}(E) = L\varepsilon_{\text{trig}}(1 - \delta_{\text{MC}}) \times \left[(1 + \delta_{\text{wid}})(1 + \delta_{\text{rad}})\sum_f \varepsilon_f^{(i)}\sigma_B^f + \sigma_{\text{bg}}^{(i)}\right]. \quad (2)$$

Here, L is the luminosity integral at the energy point; $\varepsilon_{\text{trig}}$ is the trigger efficiency; δ_{MC} is the correction to the detection efficiency; δ_{wid} is the correction taking into account the spread in the energies of the particles in the e^+e^- beams; δ_{rad} is the correction associated with the radiation of photons by the initial electrons and positrons, which is calculated according to [6]; $\varepsilon_f^{(i)}$ is the efficiency of the detection of the fth events in the ith region, $\sigma_B^f(E)$ is the cross section for the $e^+e^- \longrightarrow \phi \longrightarrow f$ ($f = \pi^+\pi^-\pi^0$, $\eta\gamma$, $\pi^+\pi^-\gamma\gamma$, $\pi^+\pi^-\eta$) reaction; and $\sigma_{\text{bg}}^{(i)}$ is the nonresonant cross section in the ith region, which is assumed to be constant. The correction values were presented in [7], where the $\phi \longrightarrow \pi^+\pi^-\pi^0$ decay was studied with the use of the same experimental data as in this analysis. The detection efficiencies $\varepsilon_f^{(i)}$ are determined through simulation [8]; the main values are presented in Table 1. The shape of the resonance curve for the last three decays of the ϕ meson is taken to be the same as for 3π, because the difference of the exact shape from the shape of the 3π cross section for each mode can be disregarded for existing statistics; i.e., $\sigma_B^f(E) = \alpha^f\sigma_B^{3\pi}(E)$($f = \eta\gamma$, $\pi^+\pi^-\gamma\gamma$, $\pi^+\pi^-\eta$). The parameters α^f and $\sigma_{\text{bg}}^{(i)}$ are obtained by minimizing the likelihood function

$$\mathcal{L}^{(i)} = 2\sum_{k=1}^{16}\left(N_{\text{calc};\,k}^{(i)} - N_k^{(i)} - N_k^{(i)}\ln\frac{N_{\text{calc};\,k}^{(i)}}{N_k^{(i)}}\right), \quad (3)$$

where $N_{\text{calc};\,k}^{(i)}$ is the expected number of events [calculated by Eq. (2)] in the ith region for the kth energy point and $N_k^{(i)}$ is the experimental number of events in the ith region for the kth energy point.

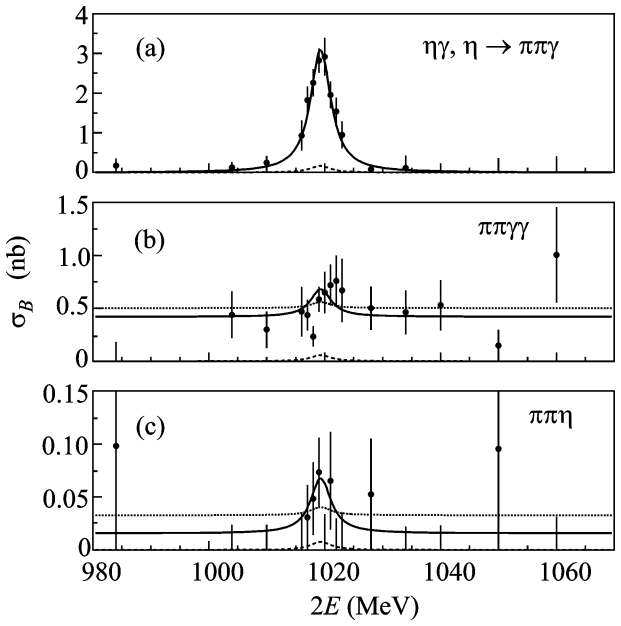

Fig. 4. Cross sections for the (a) $e^+e^- \longrightarrow \eta\gamma(\eta \longrightarrow \pi^+\pi^-\gamma)$, (b) $e^+e^- \longrightarrow \pi^+\pi^-\gamma\gamma$, and (c) $e^+e^- \longrightarrow \pi^+\pi^-\eta(\eta \longrightarrow \gamma\gamma)$ reactions. The points with the error bars are the experimental data and the solid lines are the approximations. The dashed lines in panels (a) and (b) are the resonance background from the 3π events. The dashed line in panel (c) is the resonance background from the ηγ events. The dotted lines in panels (b) and (c) are the approximation with zero resonance contribution.

The cross section in the peak σ_B^f and relative probability $\mathcal{B}^f$ of the fth decay mode are determined by the formulas

$$\sigma_B^f = \alpha^f \sigma_B^{3\pi}, \quad (4)$$

$$\mathcal{B}^f = \alpha^f \mathcal{B}^{3\pi}, \quad (5)$$

where $\mathcal{B}^{3\pi} = 0.152 \pm 0.007$ and $\sigma_B^{3\pi} = 637 \pm 28$ nb [7]. Figure 4 shows the Born cross sections for the $e^+e^- \longrightarrow \eta\gamma(\eta \longrightarrow \pi^+\pi^-\gamma)$, $e^+e^- \longrightarrow \pi^+\pi^-\gamma\gamma$, and $e^+e^- \longrightarrow \pi^+\pi^-\eta$ $(\eta \longrightarrow \gamma\gamma)$ processes along with the optimal curves. Table 2 presents the approximation results.

Table 3. Results obtained in this work in comparison with the previous measurements reported in [13, 14]

Decay	This work	Previous measurements	Theory
$\pi\pi\gamma\gamma$	$<1.2 \times 10^{-4}$	$<5 \times 10^{-4}$ [13]	1.3×10^{-4}
$\pi\pi\eta$	$<6.1 \times 10^{-5}$	$<3 \times 10^{-4}$ [13] $<1.8 \times 10^{-5}$ [14]	3.5×10^{-7}

To verify the processing procedure, the product of branching ratios (see Table 2), $\mathcal{B}(\phi \longrightarrow \eta\gamma)\mathcal{B}(\eta \longrightarrow \pi\pi\gamma) = (6.61 \pm 0.43) \times 10^{-4}$, is calculated using 285 $\phi \longrightarrow \eta\gamma(\eta \longrightarrow \pi^+\pi^-\gamma)$ events in region (ii). This value is in good agreement with the world-average value $\mathcal{B}(\phi \longrightarrow \eta\gamma)\mathcal{B}(\eta \longrightarrow \pi\pi\gamma)(\text{PDG}) = (6.10 \pm 0.18) \times 10^{-4}$ [9]. The cross sections for the $e^+e^- \longrightarrow \phi \longrightarrow \pi\pi\gamma\gamma$ and $e^+e^- \longrightarrow \phi \longrightarrow \pi\pi\eta$ processes are zero within one statistical error. The systematic errors in the $e^+e^- \longrightarrow \phi \longrightarrow \pi\pi\gamma\gamma$ and $e^+e^- \longrightarrow \phi \longrightarrow \pi\pi\eta$ cross sections are 0.041 and 0.007 nb, respectively, and are almost completely determined by the error in the estimate of the number of the background 3π events in region (iii) and ηγ events in region (iv). The upper limits are calculated using the procedure described in [10], and the total error in the cross section is calculated as the square root of the sum of the squares of the statistical and systematic errors. As a result, the upper limits $\mathcal{B}(\phi \longrightarrow \pi\pi\gamma\gamma) < 1.2 \times 10^{-4}$ and $\mathcal{B}(\phi \longrightarrow \pi\pi\eta) < 6.1 \times 10^{-5}$ (both at a C.L. of 90%) are obtained for the branching ratios of these decays. The upper limit for the $\phi \longrightarrow \pi\pi\eta$ decay is calculated taking into account that $\mathcal{B}(\eta \longrightarrow \gamma\gamma) = (39.38 \pm 0.26)\%$ [9]. The inclusion of the interference of the φ meson with higher-energy resonances in the $\pi^+\pi^-\eta$ channel on the basis of the data reported in [11, 12] does not give rise to a significant change in the upper limit for $\mathcal{B}(\phi \longrightarrow \pi\pi\eta)$.

CONCLUSIONS

The $\phi \longrightarrow \pi^+\pi^-\gamma\gamma$ and $\phi \longrightarrow \pi^+\pi^-\eta$ decays are sought in the experimental data obtained with the CMD-2 detector in the region of the φ-meson resonance. The upper limits $\mathcal{B}(\phi \longrightarrow \pi\pi\gamma\gamma) < 1.2 \times 10^{-4}$ and $\mathcal{B}(\phi \longrightarrow \pi\pi\eta) < 6.1 \times 10^{-5}$ (both at a C.L. of 90%) are determined for the branching ratios of these decays. The results are compared in Table 3 with the previous measurements and theoretical predictions.

The upper limit for the branching ratio of the $\phi \longrightarrow \pi^+\pi^-\gamma\gamma$ decay is improved by a factor of about 4 as compared to the previous CMD-2 result [13] and is somewhat lower than the theoretical prediction [3]. The upper limit for $\mathcal{B}(\phi \longrightarrow \pi\pi\eta)$ is improved by a factor of about 5 as compared to the result presented in [13], but it is almost three times higher than the other CMD-2 result from [14], where this decay was sought in the events with five pions in the final state, $\phi \longrightarrow \pi^+\pi^-\eta$, $\eta \longrightarrow \pi^+\pi^-\pi^0$. The currently measured upper limit for $\mathcal{B}(\phi \longrightarrow \pi\pi\eta)$ is still much higher than the theoretical prediction [5].

This work was supported by the Russian Foundation for Basic Research (project nos. 06-02-16156, 06-02-26590, and 06-02-16445), by INTAS (grant nos. YSF 06-100014-9464 and 05-1000008-8328), by Deutsche Forschungsgemeinschaft (grant no. GZ RUS 113/769/0-2), and by the Council of the President of the

Russian Federation for Support of Young Scientists and Leading Scientific Schools (project nos. NSh-5655.2008.2 and NSh-4837.2008.2).

REFERENCES

1. E. V. Anashkin et al., Instrum. Exp. Tech. **49**, 798 (2006).
2. V. V. Anashin, I. B. Vasserman, V. G. Veshcherevich, et al., Preprint IYaF 84-114 (Novosibirsk, 1984).
3. Pyungwon Ko, Jungil Lee, and H. S. Song, Phys. Lett. B **366**, 287 (1996).
4. E. E. Jenkins, A. V. Manohar, and M. B. Wise, Phys. Rev. Lett. **75**, 2272 (1995).
5. V. A. Karnakov, Sov. J. Nucl. Phys. **42**, 634 (1985).
6. E. A. Kuraev and V. S. Fadin, Sov. J. Nucl. Phys. **41**, 466 (1985).
7. R. R. Akhmetshin et al., Phys. Lett. B **642**, 203 (2006).
8. E. V. Anashkin et al., Preprint IYaF 99-1 (Novosibirsk, 1999).
9. W.-M. Yao et al., J. Phys. G **33**, 1 (2006).
10. G. F. Feldman and R. D. Cousins, Phys. Rev. D **57**, 3873 (1998).
11. R. R. Akhmetshin et al., Phys. Lett. B **489**, 125 (2000).
12. B. Aubert et al., Phys. Rev. D **76**, 092005 (2007).
13. R. R. Akhmetshin et al., Phys. Lett. B **434**, 426 (1998).
14. R. R. Akhmetshin et al., Phys. Lett. B **491**, 81 (2000).

Translated by R. Tyapaev